

ORIGINAL RESEARCH

LAMP2 Cardiomyopathy: Consequences of Impaired Autophagy in the Heart

Ronny Alcalai, MD,* Michael Arad , MD*; Hiroko Wakimoto, MD, PhD; Dor Yadin , MA; Joshua Gorham , BA; Libin Wang, MD, PhD; Elia Burns, PhD; Barry J. Maron , MD; William C. Roberts , MD; Tetsuo Konno, PhD; David A. Conner, PhD; Antonio R. Perez-Atayde , MD; Jon G. Seidman, PhD; Christine E. Seidman, MD

BACKGROUND: Human mutations in the X-linked lysosome-associated membrane protein-2 (*LAMP2*) gene can cause a multi-system Danon disease or a primary cardiomyopathy characterized by massive hypertrophy, conduction system abnormalities, and malignant ventricular arrhythmias. We introduced an *in-frame LAMP2 gene exon 6 deletion* mutation (denoted L2^{Δ6}) causing human cardiomyopathy, into mouse *LAMP2* gene, to elucidate its consequences on cardiomyocyte biology. This mutation results in *in-frame* deletion of 41 amino acids, compatible with presence of some defective LAMP2 protein.

METHODS AND RESULTS: Left ventricular tissues from L2^{Δ6} and wild-type mice had equivalent amounts of *LAMP2* RNA, but a significantly lower level of LAMP2 protein. By 20 weeks of age male mutant mice developed left ventricular hypertrophy which was followed by left ventricular dilatation and reduced systolic function. Cardiac electrophysiology and isolated cardiomyocyte studies demonstrated ventricular arrhythmia, conduction disturbances, abnormal calcium transients and increased sensitivity to catecholamines. Myocardial fibrosis was strikingly increased in 40-week-old L2^{Δ6} mice, recapitulating findings of human *LAMP2* cardiomyopathy. Immunofluorescence and transmission electron microscopy identified mislocalization of lysosomes and accumulation of autophagosomes between sarcomeres, causing profound morphological changes disrupting the cellular ultrastructure. Transcription profile and protein expression analyses of L2^{Δ6} hearts showed significantly increased expression of genes encoding activators and protein components of autophagy, hypertrophy, and apoptosis.

CONCLUSIONS: We suggest that impaired autophagy results in cardiac hypertrophy and profound transcriptional reactions that impacted metabolism, calcium homeostasis, and cell survival. These responses define the molecular pathways that underlie the pathology and aberrant electrophysiology in cardiomyopathy of Danon disease.

Key Words: autophagy ■ calcium transients ■ cardiomyopathy ■ Danon disease ■ mouse model

Human mutations in the lysosome-associated membrane protein-2 (*LAMP2*) gene encoded on chromosome X produce a range of severe clinical manifestations. *LAMP2* mutations that encode null alleles cause multisystem Danon disease with neurologic, hepatic, skeletal and cardiac muscle abnormalities.¹ In some patients/families, *LAMP2* mutations primarily cause cardiomyopathy, which accounts for ≈1%–3% of unexplained cardiac hypertrophy in adolescents and young men.^{2–4} *LAMP2* cardiomyopathy

exhibits ventricular hypertrophy, conduction system defects and ventricular arrhythmias,^{1,5,6} resulting in heart failure and early death in young males and in women of diverse ages. We assumed that some of these mutations lead to production of certain amounts of abnormal LAMP2 protein, thereby accounting for the phenotypic differences.²

LAMP2 is a 410 amino acid, highly glycosylated protein that together with LAMP1 constitutes about 50% of lysosomal membrane proteins. While its precise

Correspondence to: Michael Arad, MD, Leviev Heart Center, Sheba Medical Center, Sackler School of Medicine, Tel Aviv University, Ramat Gan, Israel.
E-mail: michael.arad@sheba.health.gov.il

*R. Alcalai, M. Arad, J.G. Seidman, and C.E. Seidman contributed equally.

Supplementary Material for this article is available at <https://www.ahajournals.org/doi/suppl/10.1161/JAHA.120.018829>

For Sources of Funding and Disclosures, see page 12.

© 2021 The Authors. Published on behalf of the American Heart Association, Inc., by Wiley. This is an open access article under the terms of the Creative Commons Attribution-NonCommercial-NoDerivs License, which permits use and distribution in any medium, provided the original work is properly cited, the use is non-commercial and no modifications or adaptations are made.

JAHA is available at: www.ahajournals.org/journal/jaha

CLINICAL PERSPECTIVE

What Is New?

- We developed a mouse model of Danon disease containing a mutation found in a human family; mice develop cardiomyopathy and conduction system disease comparable with cardiac manifestations in the affected humans.
- Unlike previous statements associating Danon's disease with absence of LAMP2 (lysosome-associated membrane protein-2), ie null allele, we demonstrate the presence of abnormal protein in mutant mice. In addition to accumulating autophagosomes, mice suffer from abnormal lysosomal localization and dysfunction.
- Cardiomyocytes from mutant mice demonstrate prolongation of contraction and relaxation, abnormal calcium transients and increased sensitivity to catecholamines.

What Are the Clinical Implications?

- Different effects of *LAMP2* mutations on protein expression may explain the phenotypic diversity of Danon disease.
- Presence of abnormal LAMP2 protein may give rise to a predominant cardiac phenotype.
- Physiological and pharmacological factors affecting autophagic flux may modify the clinical course of cardiomyopathy in Danon disease.

Nonstandard Abbreviations and Acronyms

CsA	cyclosporine A
L2^{Δ6}	<i>LAMP2</i> gene with <i>in-frame</i> deletion of exon 6
LAMP2	lysosome-associated membrane protein-2
LC3	microtubule-associated protein light chain 3
WT	wild-type

functions remain obscure, LAMP2 is thought to participate in lysosomal biogenesis, particularly the sequestration of enzymes, and in mediating lysosomal fusion with autophagosomes. This vesicular structure contains aged and defective cellular material targeted for autophagy, ie, degradation and recycling.^{7–9} How defects in these cellular processes result in the malignant cardiomyopathy of Danon disease is not completely understood.

A previously reported *LAMP2*-null mouse^{10–13} recapitulates the multisystem manifestations of Danon disease, demonstrating prominent accumulation of

autophagic vacuoles in visceral organs and striated muscles, resulting in early lethality.^{12,13} To study how hypomorphic *LAMP2* mutations cause cardiomyopathy, we targeted the endogenous murine *LAMP2* gene by introducing an *in-frame* deletion of exon 6 (designated L2^{Δ6}). This mutation was previously identified by us in a human family with cardiomyopathy.² We hereby report the phenotype and molecular analyses of L2^{Δ6} mice, defining novel hypertrophic pathways that are clearly distinct from molecular signals responsible for cardiac hypertrophy by sarcomere protein gene mutations or storage diseases.

METHODS

Mouse Model

Mouse studies were performed in accordance with protocols approved by the Institutional Animal Care and Use Committee of Harvard Medical School. The data that support the findings of this study are available from the first author upon reasonable request.

The mouse *LAMP2* gene was identified in murine CITB CJ7-129 Sv BAC library (Invitrogen, AI). Using ET cloning technology,¹⁴ a 10450bp fragment encoding exons 4–6 and flanking intron sequence (Figure 1A) was subcloned into a modified Bluescript vector. A KpnI-SacII fragment from PK11 vector containing the neomycin resistance gene with flanking Frt sites¹⁵ and a LoxP site was introduced into the XmaI site in intron 6. Another LoxP site was introduced by standard mutagenesis into intron 5, located 200 bp 5' of exon 6. The targeting construct (Figure 1A) was subcloned into the thymidine kinase vector between the XhoI and NotI sites.

The targeting construct was electroporated into mouse embryonic stem cells. Targeted embryonic stem cell clones were identified by Southern blot analyses: DNA was digested with SacII and probed with a fragment corresponding to 665 bases 5' of the targeting construct.

The L2^{Δ6} mice were made in 129SVEv embryonic stem cells. Germline *LAMP2*-Neo mice were sequentially bred with mice expressing Frt-recombinase (Jackson Laboratory 005703, B6. Cg-Tg(ACTFLPe)9205Dym/J) to remove the neo cassette in the germline. Then they were bred with mice expressing Cre-recombinase (Jackson Laboratory 003328, 129S/Sv-Tg(Prm-cre)58Og/J) to generate the germline deletion L2^{Δ6} mice. The recombinase transgenes were removed during multiple subsequent backcrosses into the 129S6/SvEvTac background and there was no residual Cre activity.

All experiments were performed on male mice with germline L2^{Δ6} mice or their wild-type (WT) littermates. Heterozygous females had no manifest phenotype

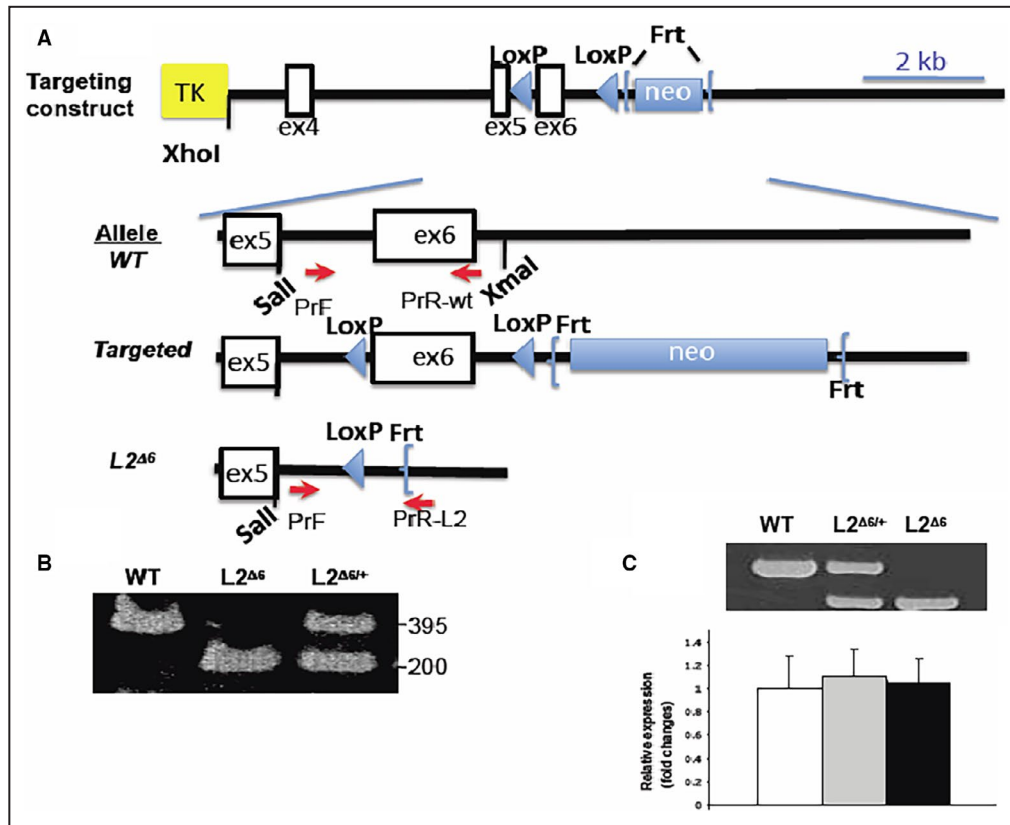


Figure 1. Construction of *in-frame* LAMP2 gene exon 6 deletion (L2^{Δ6}) mice.

A, Illustration of the L2^{Δ6} targeting construct shows the neomycin resistance gene surrounded by 2 flipase recognition target (Frt) sites with exon (ex) 6 flanked by 2 locus of X-over P1 (LoxP) sites, ligated to the thymidine kinase vector, between XhoI and NotI restriction sites. The charts below show on a larger scale the wild-type (WT) allele, the engineered allele and the final L2^{Δ6} allele after applying Frt-recombinase and Cre-recombinase. Primers used for genotyping (see Methods) are denoted by red arrows. TK, thymidine kinase; neo, neomycin resistance gene **B**, Genotypes of WT, heterozygous female L2^{Δ6/+} and male L2^{Δ6} mice were determined by size characterization of polymerase chain reaction-amplification of exon 6 using a common primer F together with R(WT) or R(L2^{Δ6}) in 1 reaction. Amplicons of a WT (395 bp), L2^{Δ6} hemizygous male (~200 bp) and of heterozygous female are shown. **C**, Lysosome-associated membrane protein-2 gene (LAMP2) reverse transcriptase-polymerase chain reaction shows L2^{Δ6} RNA shorter by 123 bases compared with the WT transcript. Both WT and L2^{Δ6} transcripts are present in female (heterozygous) heart. Sequence analyses of polymerase chain reaction products confirmed the absence of exon 6 in L2^{Δ6} transcripts (data not shown). Real-time quantitative polymerase chain reaction showed comparable levels of LAMP2 transcripts in the hearts from WT (white bar), heterozygous L2^{Δ6/+} (grey bar) and female L2^{Δ6/+} (black bar) mice, mean±SEM. L2^{Δ6} indicates *in-frame* LAMP2 gene exon 6 deletion; and WT, wild-type.

and were thus used for breeding. Mice were genotyped by polymerase chain reaction (PCR) using the following primers (denoted by red arrows Figure 1A): F-CCTCATTTGGACACCAGAGGGAGTG; R(WT)-GACAGCTGCCGGTGAAGTTGGTTG or R(L2^{Δ6})-TCACCGCGGTGGCGGCCG. To demarcate the conductive system, L2^{Δ6} mice were bred to Mink-lacZ reporter mice.¹⁶

Quantitative Real-Time Reverse Transcriptase-PCR

Two micrograms of ventricular RNA was isolated from 20- to 30-week-old L2^{Δ6}, L2^{Δ6/+} heterozygous female

and WT male mice using the TRIzol reagent (Invitrogen, Carlsbad, CA) and reverse transcribed with random hexamer primers and MultiScribe reverse transcriptase (High Capacity cDNA Reverse Transcription Kit, Applied Biosystems, Foster City, CA). Oligonucleotide primers F(LAMP2): 5'-AGGCGCAAAGCTCATCCTG-3'; R(LAMP2): 5'-CCCATTCTGCATAAAGGCAAGTA-3'; F (Hprt): 5'-GTAAAGCAGTACAGCCCCAAA-3'; R(Hprt): 5'-AGGG-CATATCCAACAACAACTT-3' were designed using Primer3 (<http://frodo.wi.mit.edu/>) or retrieved from Primer Bank (<http://pga.mgh.harvard.edu/primerbank/>). Fifteen microliter quantitative-PCR reactions were performed by 7500 Fast Real-Time PCR System (Applied Biosystems, Foster City,

CA) containing Power SYBR Green PCR Master Mix (Applied Biosystems, Foster City, CA), 7.5 pmol of each primer, and 2 μ L of cDNA template. Levels of mRNA expression were normalized using hypoxanthine guanine phosphoribosyl transferase-1 (*Hprt1*) as control and calculated according to the ΔC_T method.¹⁷ The dissociation curve analysis was performed after each complete quantitative PCR to confirm an expected DNA product.

Protein Analysis

Lysosome protein extracts were prepared using sucrose density centrifugation based on the method of Harms et al.¹⁸ Following tissue lysis in NP40-containing buffer, ventricular cytoplasmic and sarcoplasmic reticulum fractions were separated by differential centrifugation as described.¹⁹ Protein concentrations were determined by the Bradford method (Bio-Rad) or BCA assay (Pierce). Western blots of cell fractions were performed using standard procedures with the following antibodies: rabbit monoclonal anti-LAMP1 (1:500, Sigma), rabbit monoclonal anti-LAMP2 (1:500, Sigma), goat monoclonal anti-Cathepsin B (1:1000, R&D systems), goat monoclonal anti-Cathepsin D (1:1000, R&D systems), rabbit polyclonal anti-microtubule-associated protein light chain 3 (LC3)-I and LC3-II (1:1000, Cell Signaling Technology), rabbit polyclonal anti-calsequestrin (1:2500, Affinity BioReagents), mouse monoclonal anti-SERCA2 ATPase (1:5000, Affinity BioReagents), rabbit polyclonal anti-calstabin (FKBP12.6) (1:1000; Affinity BioReagents), mouse monoclonal anti-PLN (1:1000; Millipore), rabbit polyclonal anti-RyR2 DeP Ser2809 (un-phosphorylated at serine residue 2809; 1:1000; Badrilla), rabbit polyclonal anti-RYR2 P Ser2809 (phosphorylated at serine residue 2809; 1:1000; Badrilla). Horseradish peroxidase-conjugated secondary antibodies were used for chemiluminescence detection. Western blot signals were quantified using National Institutes of Health ImageJ software (<http://rsb.info.nih.gov/>). LC3 western blots were performed at baseline and after 48 hours of starvation (only drinking water was given). High-sensitivity cardiac troponin T levels were measured in serum with Elecsys STAT kit (Roche Diagnostics).

Echocardiography

Images were acquired using the Vevo 770 High-Resolution In Vivo Micro-Imaging System and RMV 707B scanhead (VisualSonics Inc.) at heart rates of 500 to 550 bpm as described.^{20,21} Images were obtained as 2-dimensional (left parasternal long and short axes) and M-mode (left parasternal short axis). Left ventricular (LV) end-diastolic diameter, LV end-systolic diameter, and wall thickness were determined by averaging measurements of 3 consecutive cardiac

cycles. LV fractional shortening (%) was calculated as (LV end-diastolic diameter – LV end-systolic diameter)/LV end-diastolic diameter \times 100. Two experienced observers who were blinded to genotypes conducted the measurements.

Electrophysiology

Multi-lead ECG recordings, electrophysiological studies, and continuous telemetry were performed as previously described,^{22,23} by 2 experienced electrophysiologists who were blinded to mouse genotypes.

Histopathology and Electron Microscopy

Mouse ventricular histology was performed after phosphate buffered saline (PBS) washes, fixation in 10% formaldehyde, and paraffin embedding. Five-micrometer sections were stained with hematoxylin and eosin, Masson trichrome and special stains. Human ventricular tissue from a male patient with LAMP2 mutation Y109Ter was fixed in formalin, and 6 μ m sections were stained (as a reference) with Masson trichrome.

Conduction system histology was performed in 25-week-old L2 ^{Δ 6} and WT hearts carrying the *MinK-LacZ* allele as described.¹⁶ β -Galactosidase activity in these hearts was detected by 5-bromo-4-chloro-3-indolyl-beta-d-galactopyranoside (X-Gal– dark blue) staining. Quantification of X-Gal positive cells was obtained using National Institutes of Health ImageJ software (<http://rsb.info.nih.gov/>). For transmission electron microscopy, ventricular myocardium from 25-week-old L2 ^{Δ 6} and WT mice (3 mice per group) were fixed with glutaraldehyde using standard protocols.

To study the effect of cyclosporine A (CsA) on left ventricular hypertrophy, 32-week-old mice (n=3/group), were injected subcutaneously 15 μ g/g of bodyweight twice per day, for 2 weeks. Echocardiographic measurements were done before and after treatment, as described.

Isolated Cardiomyocyte Studies

Adult ventricular myocytes were isolated via a Langendorff hanging heart preparation and enzymatic digestion as previously described.^{24,25} For immunofluorescence studies, the isolated myocytes were fixed in 1% paraformaldehyde and spun onto slides using Cytospin3 (Shandon). After PBS washes, myocytes were permeabilized with 0.2% Triton X-100 and blocked with 5% fetal bovine serum in PBS. Slides were incubated overnight with goat monoclonal antibodies against lysosomal enzymes anti-Cathepsin B (1:50, R&D systems) or anti-Cathepsin D (1:50, R&D systems) in 1% fetal bovine serum. Slides were washed and incubated with Alexa fluor 488 or 594 fluorescence labeled rabbit anti goat antibodies (1:100, Invitrogen), counterstained with Alexa Fluor 488 or

647 fluorescence labeled phalloidin (Invitrogen) and DAPI. Images were acquired using a Leica TCS SP2 confocal microscope.

For calcium transient analysis, the isolated ventricular myocytes were loaded with 1.2 mmol/L Ca^{2+} and 1 $\mu\text{mol/L}$ fura-2/AM Ca^{2+} indicator (Invitrogen) as previously described.^{23,26} Only rod-shaped cells with striations and resting sarcomere length $>1.6 \mu\text{m}$ were studied. Myocytes were quiescent in the absence of electrical stimulation or were paced with 1 Hz using platinum wires. Sarcomere contraction and fura-2 fluorescence ratios were simultaneously recorded from discrete positions in myocytes using a dual-excitation fluorescence imaging/contractility recording system (IonWizard SarcLen detection and PMT Acquisition fluorescence system; IonOptix Corp.). Sarcomere length and Ca^{2+} transient recordings were performed in Tyrode buffer, and where indicated, with 5.5 mmol/L Epinephrine using IonOptix transient analysis software (version 5.0; IonWizard).

RNA Sequence

RNAseq libraries were constructed as described,²⁷ except for libraries not normalized with the Duplex-specific enzyme or fragmented. Reads were aligned on the mouse genome using TOPHAT and BOWTIE and expression profiles were constructed as previously described.²⁷

Statistical Analysis

Data are expressed as mean \pm SEM. Significance was assessed using ANOVA, unpaired Student's *t* tests for continuous variables and Fisher exact test for categorized variables, as appropriate. Generalized Estimating Equation was used when numerous myocytes or sections were analyzed from the same mouse. *P* values <0.05 were considered significant. A change in gene expression was defined by at least ≥ 1.5 or <0.67 ratio in the read count (for increase or decrease respectively, at a *P* value of <0.001).

RESULTS

The *in-frame* exon 6 deletion in the endogenous *LAMP2* gene (Figure 1A and 1B) resulted in neonatal death in $\approx 25\%$ of hemizygous male $L2^{\Delta 6}$ mice. Surviving mutant males, while initially smaller than WT littermates, achieved comparable size and weight by 12 weeks of age (≈ 30 g), and exhibited normal voluntary activity and survival (Figure S1).

LV tissues from $L2^{\Delta 6}$ and WT mice had equivalent amounts of *LAMP2* RNA, although the $L2^{\Delta 6}$ transcript was smaller due to the deletion of 123 bp encoding exon 6 (Figure 1C). Western blots of LV extracts (Figure 2A)

showed significantly lower levels of LAMP2 protein in $L2^{\Delta 6}$ compared with WT mice (5.6-fold \pm 2.6; $P=0.002$). SDS-PAGE gels indicated that mutant and WT LAMP2 protein had comparable sizes (≈ 110 kd), implying that both molecules underwent post-translational glycation.

Development of Cardiomyopathy in $L2^{\Delta 6}$ Mice

Significant cardiac hypertrophy developed after 20 weeks of age in male $L2^{\Delta 6}$ mice (Figure 2B) with preserved or even increased systolic function (Table 1). These mice had a pronounced elevation of serum cardiac troponin T (484 \pm 246, range 150-920 ng/L, compared with non-detectable levels (<13) in WT, $P=0.001$, $n=7$ /group) indicating an ongoing myocardial injury. The fractional shortening decreased in aged (≈ 40 weeks) compared with younger $L2^{\Delta 6}$ mice while it did not change with aging in WT animals (Table 1). Heart to body weight at 40 weeks increased in $L2^{\Delta 6}$ compared with WT mice (7.44 and 6.03, respectively; $n=6$, $P<0.05$) and myocardial fibrosis was strikingly increased (Figure 2C), recapitulating findings of human LAMP2 cardiomyopathy (Figure 2D). Cell death in $L2^{\Delta 6}$ was indicated by troponin elevation and degenerative changes in some cardiomyocytes (Figure S2), and was presumably followed by myocardial fibrosis.

Hearts of $L2^{\Delta 6}$ mice contained ≈ 2 glycogen compared with WT. This accumulation is insufficient to be considered "storage"²⁸ and no PAS-positive inclusions were identified in histological sections from $L2^{\Delta 6}$ mice. Transmission electron microscopy of LV specimens from WT and $L2^{\Delta 6}$ showed that mutant myocytes had abundant bilayer membrane vesicles containing inclusions composed of cytoplasmic remnants, partially degraded organelles, and nonspecific amorphous materials. These features characterize autophagosomes, a cytoplasmic structure that deliver sequestered cargo to lysosomes for final degradation and recycling (Figure 2E). These large structures disrupted the normal sarcomere organization in $L2^{\Delta 6}$ mice (Figure 2E, right lower panel).

Heart rhythm telemetry demonstrated no difference in average sinus heart rate between WT and $L2^{\Delta 6}$ mice (data not shown). Cardiac electrophysiology showed PR prolongation and intermittent atrio-ventricular block in $L2^{\Delta 6}$ compared with WT mice (Figure 3A and 3B). Atrio-ventricular block occurred in 60% of $L2^{\Delta 6}$ and 8% of WT mice ($P=0.02$). $L2^{\Delta 6}$ mice did not exhibit ventricular pre-excitation or spontaneous arrhythmias but pacing induced ventricular arrhythmias in 75% of $L2^{\Delta 6}$ mice (but in $<10\%$ WT mice; $P=0.01$). We then assessed whether fibrosis contributed to electrophysiological abnormalities by examining the histopathology of compound $L2^{\Delta 6}$ /MinK-LacZ mice that selective express β -galactosidase in their cardiac conduction

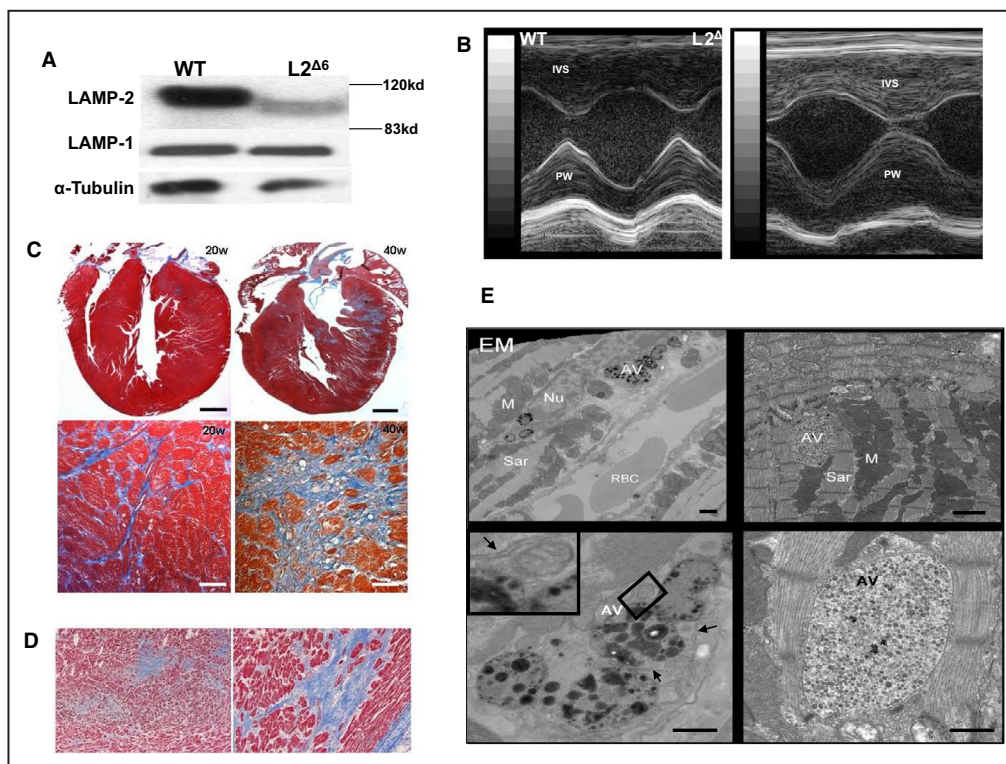


Figure 2. In-frame *LAMP2* gene exon 6 deletion ($L2^{\Delta 6}$) decreases *LAMP2* levels and causes cardiomyopathy.

A, Western blots revealed reduced *LAMP2* but normal *LAMP1* levels in lysosomal extracts from $L2^{\Delta 6}$ hearts compared with wild-type (WT) hearts ($n=4$ per genotype). The smaller $L2^{\Delta 6}$ protein reflected deletion of 41 amino acids encoded by exon 6. **B**, Echocardiograms show prominent hypertrophy of the intra-ventricular septum and posterior wall in 25-week $L2^{\Delta 6}$ mice, see also Table 1. **C**, Progressive fibrosis in $L2^{\Delta 6}$ heart. At 20-weeks, fibrosis (stained blue) is interstitial, but by 40weeks hearts show both interstitial and areas of scarring. Focal fibrosis surrounds residual $L2^{\Delta 6}$ myocytes with vacuoles. Upper panels, scale=500 mm lower panels, scale=50 mm. **D**, Heart section from a 14-year-old human patient with *LAMP2* cardiomyopathy (Y109Ter mutation) who died suddenly (Maron et al 2009⁵) demonstrating marked interstitial and replacement fibrosis (Masson trichrome). **E**, Electron microscopy (EM) of heart from 25-week-old $L2^{\Delta 6}$ mice show large autophagic vacuoles that are interspersed among sarcomeres, containing partially degraded particles. Upper panels, scale=1 mm, lower panels, scale=500 nm. Autophagic vacuoles typically have double membrane (marked with black arrows) as shown more in details in the inset of the left lower panel. AV indicates autophagic vacuoles; IVS, intra-ventricular septum; $L2^{\Delta 6}$, in-frame *LAMP2* gene exon 6 deletion; PW, posterior wall; RBC, red blood cells; and WT, wild-type.

system myocytes.¹⁶ Compound mutant mice showed marked fibrotic encasement and vacuolation of the atrio-ventricular node, less conduction system myocytes and disorganization of the proximal bundle of His (Figure 3C and 3D).

Functional Assessment of Autophagy in $L2^{\Delta 6}$ Myocytes

We used western blot analysis to assess the levels of microtubule-associated protein light chain 3 (LC3-II), which demarcates autophagosome,²⁹ the pre-lysosomal fusion step of autophagy. Mice were studied in a fed state to assess basal levels of autophagy and after food deprivation to stimulate autophagy. Compared with WT, LC3-II levels were substantially

greater in hearts from fed $L2^{\Delta 6}$ mice and comparable to levels found after 24 hours of food-deprived WT mice (Figure 4A and 4B). Food deprivation further increased LC3-II levels in $L2^{\Delta 6}$ mice, implying that $L2^{\Delta 6}$ mice retained a capacity for further increases in the basal stages of the autophagic pathway.

To assess lysosome function in $L2^{\Delta 6}$ mice, we capitalized on transcription data that indicated increased expression of 6 cathepsins (A-D, L and Z). Using Western blot analyses of LV extracts we examined protein levels of cathepsins B and D. Both were increased in cytoplasmic fractions and diminished in lysosomal fractions of LV extracts from $L2^{\Delta 6}$ hearts while the reverse was found in LV extracts from WT hearts (Figure 4C). Immunofluorescent labeling of

Table 1. Cardiac Size and Function of L2^{Δ6} Mice

	L2 ^{Δ6}		WT		ANOVA		
	Adult	Aged	Adult	Aged	Mutant	Age	Interaction
Age (w)	Adult 25.1±2.3	Aged 39.7±6.5	Adult 28.5±1.7	Aged 37.5±6.5			
n	6	6	5	8			
IVSd (mm)	0.79±0.09	0.92±0.10	0.60±0.05	0.71±0.06	0.03	0.17	0.92
LVPWd (mm)	0.97±0.05	0.99±0.10	0.70±0.05	0.82±0.05	0.006	0.35	0.5
LVEDd (mm)	3.93±0.18	4.37±0.60	3.70±0.28	3.85±0.22	0.3	0.46	0.72
FS (%)	39.3±4.9*	26.7±6.1*	31.2±3.7	32.5±4.5	0.8	0.31	0.2

Mice were studied at 2 age categories. All measurements were performed at heart rate of 500 to 550 bpm. L2^{Δ6} mice tended to have slower heart rate, but that was not statistically significant. There was no apparent difference in the negative chronotropic effect of the anesthesia between mutant and wild-type mice.

Data are expressed as mean±SEM. FS indicates fractional shortening; IVSd, interventricular septum diameter; L2^{Δ6}, *in-frame LAMP2* gene exon 6 deletion; LVEDd, left ventricular end-diastolic diameter; LVPWd, left ventricular posterior wall diameter; and WT, wild-type.

ANOVA indicates a significant increase in the wall thickness in mutant mice without effect on left ventricular dimension or shortening fraction. There was no significant effect of age or interaction of age with L2^{Δ6} mutation.

*In a post-hoc analysis, aging was associated with a decrease in the shortening fraction of L2^{Δ6} mice (**P*<0.01 comparing aged to young L2^{Δ6} mice) but no such change was seen in wild-type mice.

cathepsin B and cathepsin D identified a perinuclear location in 83% of WT myocytes (18 myocytes from 3 mice) but in only 25% of L2^{Δ6} myocytes (16 myocytes from 3 mice, *P*<0.01). Cathepsin immunofluorescence in L2^{Δ6} myocytes was more diffuse within the cytosol (Figure 4D), suggesting mis-localization of lysosomal enzymes.

In summary, transcriptional and functional analyses indicated significantly activated molecular signals that promote autophagosome and lysosome production and autophagy in L2^{Δ6} hearts. Despite these signals, there was an accumulation of autophagosome and mislocalization of lysosome enzymes in L2^{Δ6} hearts, defining a block in autophagy at the step of formation of autolysosomes.

Transcriptional Analysis in L2^{Δ6} Hearts

We then performed RNAseq²⁷ of LV tissues from 26- to 30-week-old L2^{Δ6} and WT mice, to identify transcriptional responses to the L2^{Δ6} mutation (illustrated for LAMP2 expression in Figure S3). The full results of the transcriptome analysis are provided at: <https://www.ncbi.nlm.nih.gov/geo/query/acc.cgi?acc=GSE166731> (GEO accession number GSE166731). Among the LV transcripts that were significantly altered in L2^{Δ6} mice (4.0%, increased; 2.2% decreased), there was a significant upregulation of transcripts annotated in autophagy and apoptotic pathways (Table S1). Thus, among 793 mouse homologues of yeast autophagy genes that are expressed in the LV, 62 were increased (7.8%, *P*<0.001) in L2^{Δ6} compared with WT mice and among 1252 apoptotic markers, 85(6.8%) were increased (*P*<0.001). Similarly, among 399 human autophagy network proteins³⁰ that are expressed in the LV, 86 were significantly increased in L2^{Δ6} in comparison with WT hearts (*P*<0.0001).

The main genes in the autophagy and apoptotic pathways altered in L2^{Δ6} mice compared with WT are shown in Table S2.

Abnormal Relaxation and Altered Calcium Homeostasis in L2^{Δ6} Myocytes

To assess whether impaired autophagy altered an intrinsic contractile function and calcium homeostasis, we studied isolated myocytes from 20-week-old L2^{Δ6} and WT mice (Figure 5 and Table 2). Despite accumulations of autophagosomes among sarcomeres in mutant cardiomyocytes (Figure 2A), the extent of shortening or relaxation was not different compared with WT (Figure 5A). However, the durations of contraction and relaxation were markedly prolonged in L2^{Δ6} myocytes (Table 2).

Ca²⁺ transient studies revealed prominent abnormalities in L2^{Δ6} myocytes. The mean amplitude of Ca²⁺ transients was strikingly higher in L2^{Δ6} (0.71±0.24) than in WT (0.45±0.15) myocytes (Table 2 and Figure 5A). Catecholamines further increased mean Ca²⁺ transient amplitudes to levels that were significantly higher than those found in catecholamine-stimulated WT myocytes (Figure 5B). Catecholamines also produced spontaneous and frequent sarcoplasmic reticulum Ca²⁺ release events in ≈75% of L2^{Δ6} myocytes (Figure 5C); these events were triggered in only 8% of WT myocytes (*P*=0.009).

Ca²⁺ decay in L2^{Δ6} myocytes was slower than in WT myocytes (Table 2). However, because catecholamines did normalize Ca²⁺ decay times in mutant myocytes (Table 2), we deduced that the sarcoplasmic reticular pump, Ca²⁺-ATPase (Serca2a), remained functional in L2^{Δ6} myocytes.

We also tested if abnormal Ca²⁺ homeostasis is associated with altered expression of Ca²⁺-handling

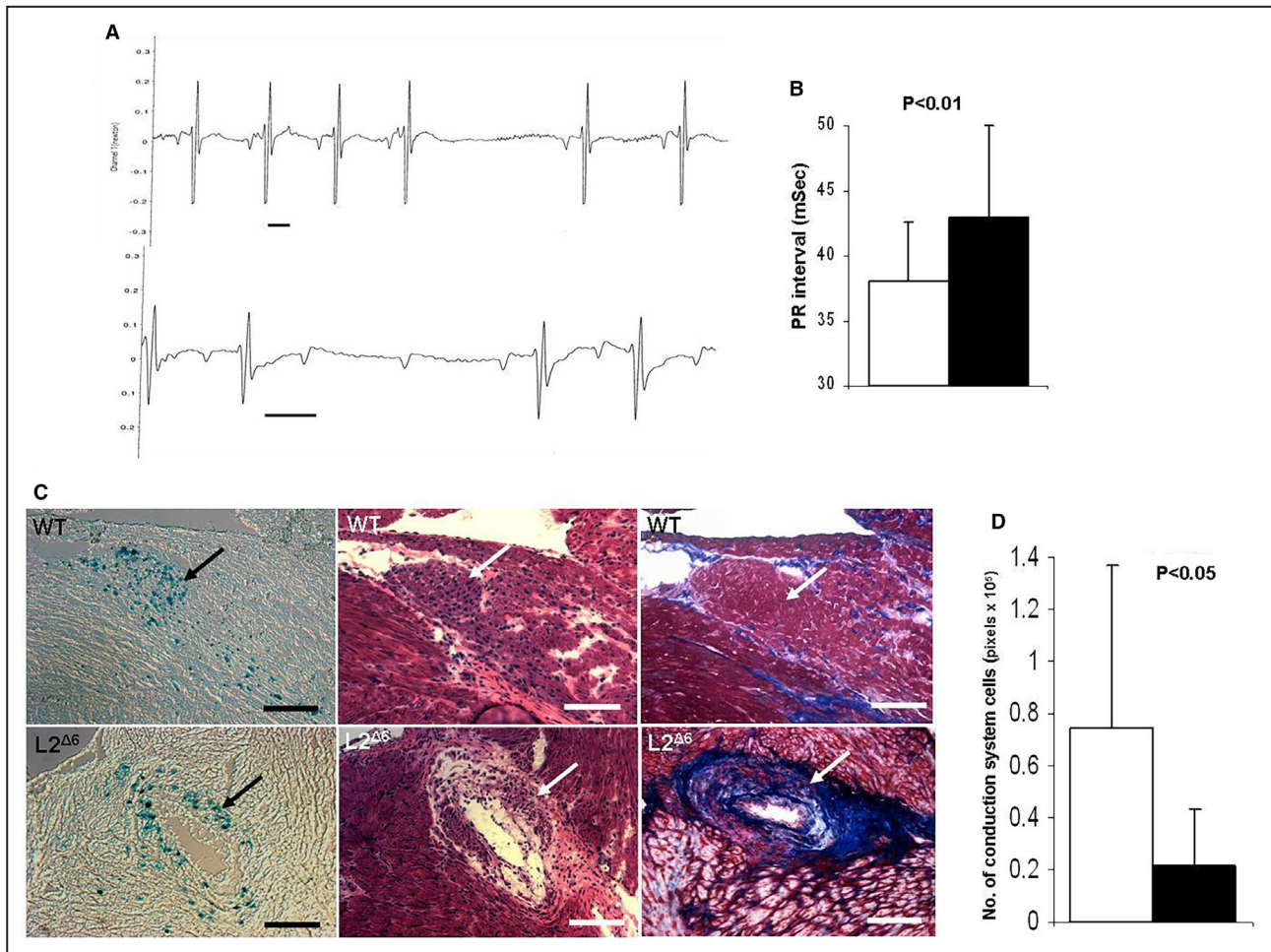


Figure 3. Conduction system physiology and histology of *in-frame* LAMP2 gene exon 6 deletion ($L2^{\Delta 6}$) hearts.

A, Representative traces recorded by telemetry in 15-week-old $L2^{\Delta 6}$ mice: upper panel showed transient sinus node arrest and middle panel shows transient atrioventricular block, Scale bars represent 50mSec. **B**, Average PR intervals (the time from the onset of the P wave to the start of the QRS complex on the electrocardiogram) of 15 weeks old WT (white bar) and $L2^{\Delta 6}$ (black bar) mice, $n=10$ /genotype, mean \pm SEM. **C**, Histology of the atrioventricular node and surrounding tissues in 15-week-old MnK/WT mouse (upper panels) and MnK/ $L2^{\Delta 6}$ mouse (lower panels). The hearts were stained with X-Gal to identify β -galactosidase activity in the conduction system cells (Blue dots in left panels), and then counterstained with hematoxylin–eosin (middle panels) and with Masson Trichrome (right panels). The atrioventricular node (arrow) in the MnK/ $L2^{\Delta 6}$ hearts was more disorganized than MnK/WT hearts. Fibrosis and large vacuoles were detected in the atrioventricular region of MnK/ $L2^{\Delta 6}$ but not in the MnK/WT hearts. Scale bars represent 200 μ M. **D**, Quantitation of positive X-Gal staining which represents conduction system cells. MnK/ $L2^{\Delta 6}$ hearts had less conduction cells (black bar) compared with MnK/WT (white bar). Analysis was done in consecutive section containing the atrioventricular node from 4 mice aged 15 to 20 weeks of each genotype, 3 sections per heart. Generalized Estimating Equation was used for statistical comparison. $L2^{\Delta 6}$ indicates *in-frame* LAMP2 gene exon 6 deletion; and WT, wild-type.

proteins. Transcripts encoding the cardiac ryanodine receptor (RyR2) and the RyR2-stabilizing protein FKBP12.6 showed coordinate increase above their levels in WT mice (both with $P<0.0001$). In contrast, transcript levels of SERCA2 and PLN (phospholamban) were unchanged while the expression of the sarcoplasmic reticulum calcium binding proteins CASQ1/2 (calsequestrin), were decreased. As predicted from RNA data, protein levels of the cardiac ryanodine receptor were increased in $L2^{\Delta 6}$ hearts as were the levels

of phosphorylated cardiac ryanodine receptor (pRyR2, Figure 5D). On the other hand, the levels of SERCA2a, total PLN, phosphorylated PLN, and CASQ2 were comparable between $L2^{\Delta 6}$ and WT hearts (Figure S4A), similar to LAMP2-null hearts.¹² Collectively, a marked increase in ryanodine receptor phosphorylation (pRyR2) in $L2^{\Delta 6}$ hearts, unopposed by FKBP12.6 (Figure 5D and Figure S4B), would promote increased Ca^{2+} leak from the RyR2 and might account for delayed after-depolarizations and arrhythmias.

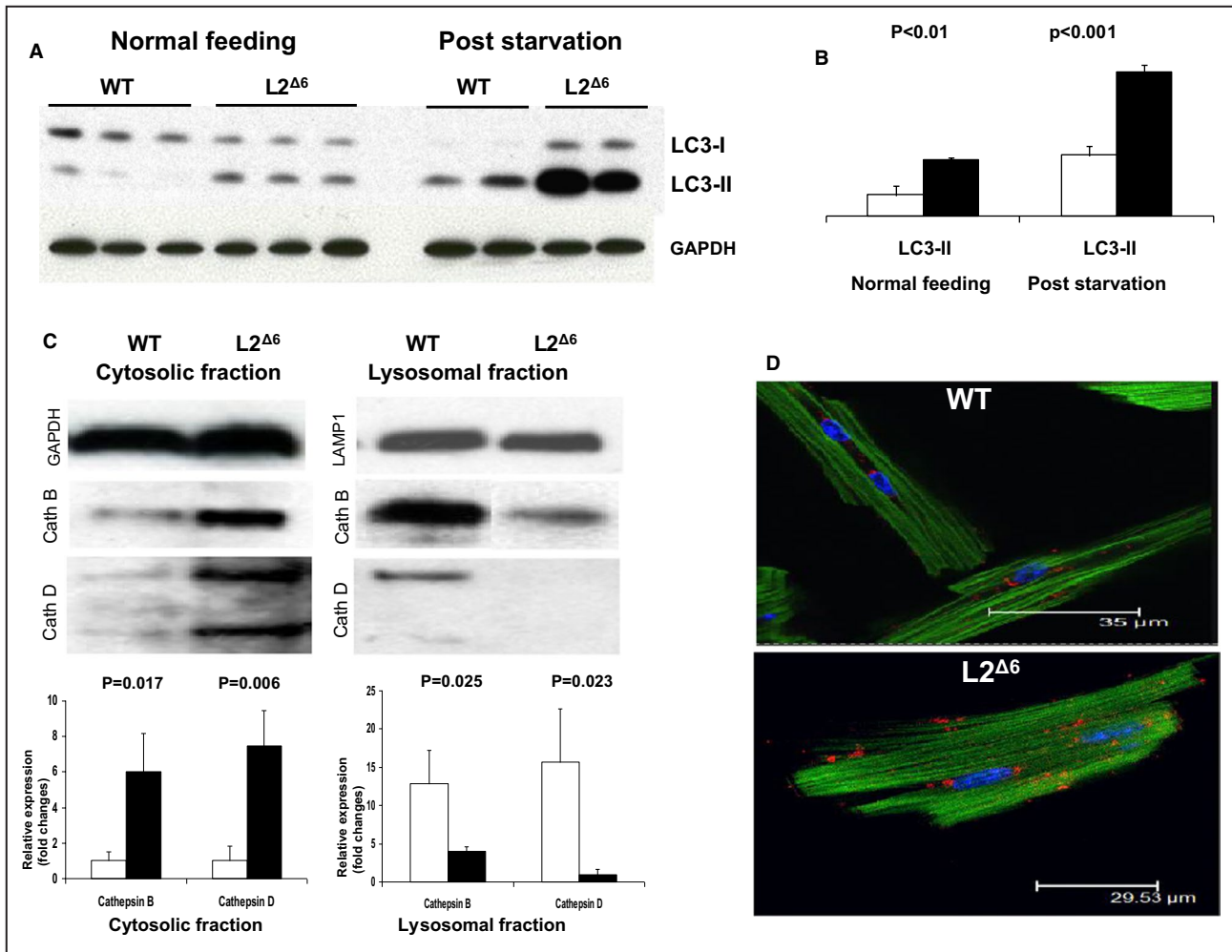


Figure 4. Disrupted autophagy in *in-frame* LAMP2 gene exon 6 deletion ($L2^{\Delta 6}$) hearts.

A, Western blot analysis of the microtubule-associated protein light chain 3 (LC3) extracted from 20-weeks old wild-type (WT) and $L2^{\Delta 6}$ mice hearts. Upper band represent the LC3-I, which is cytosolic, and the lower LC3-II is present on isolation membranes and autophagosomes. **B**, Densitometry (3 mice of each genotype) shows that $L2^{\Delta 6}$ hearts (black bars) express higher levels of LC3-II compared with WT (white bars). Markedly increased LC3-II levels after starvation indicate farther accumulation of autophagosomes. **C**, Western blot of lysosomal enzymes cathepsin B and D in fractionated subcellular extracts. Densitometry (3 mice of each genotype) shows increased levels of cathepsin B and D in the cytosolic fraction of $L2^{\Delta 6}$ hearts (black bars) compared with WT (white bars) and reciprocally decreased levels in the lysosomal fractions. **D**, Representative confocal micrographs of WT and $L2^{\Delta 6}$ myocytes stained with immunofluorescent anti-Cathepsin B antibody (red), DAPI (blue) and Phalloidin (green). Note a peri-nuclear localization of lysosomes detected by the anti-cathepsin antibody in WT myocytes. Cathepsin immunofluorescence is dispersed throughout the cytoplasm in $L2^{\Delta 6}$ myocytes. Numerical data are expressed as mean \pm SEM. $L2^{\Delta 6}$ indicates *in-frame* LAMP2 gene exon 6 deletion; LC3, microtubule-associated protein light chain 3; and WT, wild-type.

Hypertrophic Signaling

Cardiac hypertrophy in $L2^{\Delta 6}$ mice was associated with alteration in gene expression related to myocardial stretch and various forms of hypertrophic remodeling. Genes such as *nppb* (x4.2), *nppa* (x3.8) and *acta1* (x2.5), markedly and significantly increased (all at $P<0.0001$). Because increased frequency of spontaneous Ca^{2+} transients could also affect molecular signaling through either the calcineurin/NFAT (Nuclear factor of activated T-cells) pathway³¹ or by mitochondrial autophagy we

hypothesized that calcineurin³² might have an effect on $L2^{\Delta 6}$ cardiomyopathy. Indeed, calcineurin RNA (*ppp3ca*) is increased 1.4-fold ($P=0.0008$) in $L2^{\Delta 6}$ left ventricles. We therefore treated adult $L2^{\Delta 6}$ mice with CsA that blocks mitochondrial autophagy and modulates cardiac hypertrophy. After 2 weeks of CsA treatment, there was a reduction in LV wall thickness in $L2^{\Delta 6}$ hearts compared with untreated mice (Figure S5). However, neither the fractional shortening, nor the fibrosis burden, were affected by CsA treatment.

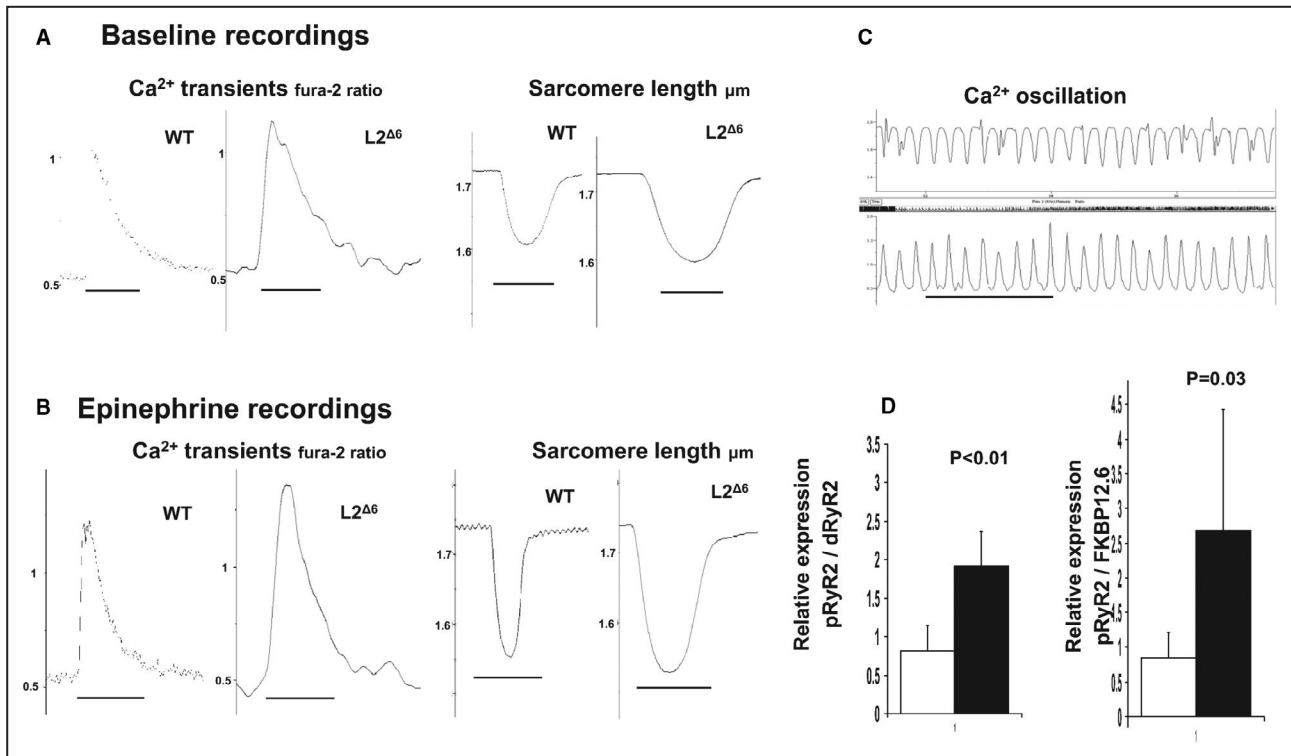


Figure 5. Ca²⁺ abnormalities in *in-frame* LAMP2 gene exon 6 deletion cardiomyocytes.

A, B, Representative calcium (Ca²⁺) transients (left panels) and sarcomere length (right panels) of wild-type and *in-frame* Lysosome-associated membrane protein-2 gene (*LAMP2*) gene exon 6 deletion myocytes in Ca²⁺ Tyrode solution without (a) or with (b) 5.5 mmol/L epinephrine. Traces represent the average of 15 contraction-relaxation cycles at 1 Hz from 1 representative cell of each genotype. **C,** Epinephrine infusion produced spontaneous Ca²⁺ oscillations *in-frame* LAMP2 gene exon 6 deletion myocytes (sarcomere length, upper trace; Ca²⁺ transient, lower trace). Scale=0.2 sec. **D,** Quantitative Western blot estimate of phosphorylated ryanodine receptor 2 (pRyR2) in SR extracts from *in-frame* LAMP2 gene exon 6 deletion (black bar) and wild-type (white bar) hearts. The relative amounts of pRyR2, de-phosphorylated ryanodine receptor 2 (dRyR2), and FK506 binding protein 12.6 (FKBP12.6, calstabin-2) were determined by densitometry of antibody signals (n=3 mice/group, mean±SEM). See Table 2 for comparisons. L2^{Δ6} indicates *in-frame* LAMP2 gene exon 6 deletion; SR, sarcoplasmic reticulum, and WT, wild-type.

DISCUSSION

L2^{Δ6} mice expressing a defective LAMP2 allele missing the 41 amino acids of exon 6, constitute a useful model recapitulating the human cardiomyopathy associated with Danon disease. L2^{Δ6} hearts contain considerably less LAMP2 protein than WT hearts in the presence of normal mRNA levels (Figure 1C), suggesting that the mutant LAMP2^{Δ6} protein is unstable (Figure 2). Whether cardiomyopathy results from reduced amounts of protein or altered activity of the mutant protein remains uncertain. Nevertheless, the fact that in the presence of certain amounts of protein, L2^{Δ6} mice appear to have a better survival compared with the null-allele LAMP2 mice,¹⁰ suggests that the expressed mutant protein retains some of its function. Further, deficiency in mutant protein, rather than its toxic effect, is responsible for the phenotype. As opposed to a complete LAMP2 gene deficiency,¹⁰ the hypomorphic LAMP2 allele in L2^{Δ6} mutant mice allow the animals to survive to adulthood and develop significant cardiomyopathy.

Characterization of the cardiac phenotype of L2^{Δ6} mice provides further insights into the mechanisms of LAMP2-mediated cardiomyopathy. L2^{Δ6} mice demonstrate that lysosomal dysfunction appears to be a powerful stimulus for hypertrophic remodeling, heart failure, and cardiac arrhythmias. Of the multiple ensuing consequences, failed autophagy appears to be a fundamental cause of progressive cardiomyopathy. Studies demonstrating that activation of autophagy can ameliorate load-induced hypertrophy³¹ support our conclusion. This pathway differs from "hypertrophic" sarcomere protein mutations that enhance contractile parameters,³² structural protein mutations (eg, desmin, alphaB-crystallin, ZASP) that accumulate abnormal protein aggregates,³³ or defects in metabolic genes accrue glycogen, glycolipids, or their degradation products (eg, *PRKAG2*,³⁴ *GAA*³⁵ *GLA*).³⁶ Importantly, there is a growing appreciation of the role of a secondary dysfunction of autophagy in pathophysiology of lysosomal storage diseases.³⁷ Unlike in the original description of Danon disease defining it as "Pompe"

Table 2. Cardiomyocytes Properties in L2^{Δ6} Mice

	WT	L2 ^{Δ6}	P Value
Isolated myocytes*			
Resting myocyte length (μm)	1.75±0.06	1.76±0.05	NS
% Sarcomere shortening	6.6±2.1	7.4±2.8	NS
Time to 50% contraction (mSec)	25±7	65±15	<0.001
Time to 50% relaxation (mSec)	148±40	310±80	<0.001
Ca ²⁺ transient amplitude (Fura2 ratio)	0.45±0.15	0.71±0.24	<0.001
Time to 50% transient decay (mSec)	118±13	201±69	<0.001
Ca ²⁺ transient decay–Tau (mSec)	124±22	178±52	<0.001
Catecholamine stimulated myocytes†			
Resting myocyte length (μm)	1.72±0.06	1.73±0.06	NS
% Sarcomere shortening	12.9±3.3	13.5±3.7	NS
Time to 50% contraction (mSec)	20±4	32±13	<0.05
Time to 50% relaxation (mSec)	107±18	150±50	<0.05
Ca ²⁺ transient amplitude (Fura2 ratio)	0.56±0.17	0.92±0.3	<0.01
Time to 50% transient decay (mSec)	92±16	105±25	NS
Ca ²⁺ transient decay–Tau (mSec)	68±9	69±17	NS

Data are expressed as mean±SEM. L2^{Δ6} indicates *in-frame* LAMP2 gene exon 6 deletion; LAMP2, lysosome-associated membrane protein-2; NS, non-significant; and WT, wild-type.

*Sarcomere lengths and shortening of myocytes (n=21 and n=29 cells from 4 wild-type (WT) and 5 *in-frame* LAMP2 exon 6 deletion (L2^{Δ6}) mice, respectively). Ca²⁺ transients were measured in myocytes (n=30 cells and n=18) from 5 WT and 3 L2^{Δ6} mice, respectively.

†Catecholamine-stimulated sarcomere lengths and shortening were measured in myocytes (n=11 and n=10) from 4 WT and 3 L2^{Δ6} mice, respectively. Catecholamine-stimulated Ca²⁺ transients were measured in myocytes (n=12 and n=12 cells from 4 WT and 3 L2^{Δ6} mice, respectively).

with normal acid maltase or GSD IIb, we did not find evidence of significant glycogen storage. That could result from differences in glycogen metabolism and lower levels of glycogen in murine heart compared with humans.²⁸ Differences in glycogen accumulation could explain why humans but not mice with Danon disease often develop massive left ventricular hypertrophy.

The L2^{Δ6} mutation causes incomplete lysosome biogenesis. Lysosomes in L2^{Δ6} myocytes had mistargeting of cathepsins B and D and glycolytic enzymes. Consistent with these markers of incomplete maturation, L2^{Δ6} lysosomes were dispersed throughout the cytosol (Figure 4), whereas normal lysosomes clustered in perinuclear regions. Autophagosomes containing

aggregated proteins and membrane components accumulated in L2^{Δ6} myocytes. The expression of 62 RNAs encoding autophagy-associated proteins was increased. More importantly LC3-II, a marker of autophagosomes, was significantly overexpressed in L2^{Δ6} hearts compared with WT (Figure 4). Processing of autophagosome requires docking and fusion with mature lysosomes, to yield phagolysosomes that move via microtubules to perinuclear regions.³⁸ Collectively, autophagy appears to be stimulated in L2^{Δ6} myocytes, but the later stages in the process are blocked, resulting in accumulated autophagosomes, absent phagolysosomes, and myocytes unable to clear cellular debris or effectively recycle proteins and organelles. Myocytes from fasted L2^{Δ6} mice expressed significantly more LC3-II than myocytes from non-fasted L2^{Δ6} mice. These results indicate that food deprivation, an autophagy-stimulating stress, causes additional autophagosome accumulation and may be expected to aggravate cardiac disease in L2^{Δ6} animals. To summarize, tissue injury and hypertrophy in L2^{Δ6} mice probably triggered by accumulation of autophagosomes and multiple partially degraded cytosolic organelles. Failed autophagy apparently promotes myocyte apoptosis³⁹ (Table S1) or necrosis, which are followed by fibrosis and arrhythmogenicity.

Additional mechanisms likely contribute to development of LAMP2 cardiomyopathy. Activation of hypertrophy associated genes indicate myocardial stretch in hypertrophic signaling. Recent studies confirm the critical role of defective mitophagy, oxidative stress, and energetic deficiency in the pathogenesis of LAMP2 cardiomyopathy.^{40–42} CsA attenuates cardiac hypertrophy caused by pressure overload but aggravates it when caused by sarcomere protein gene mutations.^{32,43} Carreira et al reported that changes in mitochondrial membrane permeability under stress conditions can trigger autophagy, a process called mitochondrial permeability transition.⁴⁴ Because CsA is a potent inhibitor of the Ca²⁺-dependent pore in heart mitochondria,⁴⁵ it could block mitochondrial permeability transition and autophagy in cardiomyocytes. Treatment of adult L2^{Δ6} mice with CsA, a calcineurin inhibitor, results in attenuation of cardiac hypertrophy without affecting systolic function or decreasing fibrosis (Figure S5). These data do support the involvement of calcineurin/NFAT (Nuclear factor of activated T-cells) pathway⁴³ in cardiac remodeling in Danon disease. It is possible that the effect of CsA could be more pronounced if given in younger mice before development of cardiomyopathy and fibrosis.

Another prominent feature of LAMP2 cardiomyopathy is conduction block, which was associated in our model with infiltration and pathological alterations in the conduction system (Figure 3). The death of L2^{Δ6} myocytes could arise from toxic accumulations

autophagosomes and/or energy deficits. Additionally, the absence of recycling of subcellular components would necessitate that L2^{Δ6} myocytes to expend more energy on de novo protein synthesis. While the long-term survival of most L2^{Δ6} mice indicated that cardiomyocyte death and energy deficits were tolerable to a certain extent, these parameters likely contribute to the uniform progression of human LAMP2 cardiomyopathy to heart failure.

Both humans with LAMP2 cardiomyopathy and L2^{Δ6} mice exhibit ventricular arrhythmias. Although fibrosis is thought to be one cause of such arrhythmias, L2^{Δ6} mice exhibit ventricular arrhythmias early in life even before developing fibrosis (Figure 2), suggesting that other mechanisms are likely involved in arrhythmia induction. An unexpected property of L2^{Δ6} myocytes helps to explain this conundrum: L2^{Δ6} myocytes had markedly increased Ca²⁺ transient amplitudes, prolonged contraction and relaxation times, despite having normal sarcomere shortening (Table 2, Figure 5). Augmented Ca²⁺ transients mediated by the RyR2 channel activation may evolve in L2^{Δ6} myocytes to allow these cells to maintain their contractility despite ultrastructural damage. Unfortunately, these compensatory changes in Ca²⁺ management cause the myocytes to become electrically unstable. Ca²⁺ signals are likely to account for increased ventricular arrhythmogenicity in L2^{Δ6} mice. Because mutant mice developed arrhythmias before histopathologic abnormalities and isolated L2^{Δ6} myocytes had spontaneous Ca²⁺ oscillations upon catecholamine stimulation (Figure 5C), arrhythmogenicity appears to be a fundamental property of L2^{Δ6} myocytes, and not a secondary response to hypertrophy and fibrosis.

Notably, Ca²⁺ transients in L2^{Δ6} myocytes were substantially bigger than those triggered by sarcomere gene mutations⁴⁶ possibly explaining the more severe arrhythmic phenotypes seen in patients with LAMP2 mutations compared with arrhythmias observed in patients with hypertrophic cardiomyopathy. Hyperphosphorylation of RyR2 channels, observed in L2^{Δ6} mice, is a key feature, implicating Ca²⁺ leak from the sarcoplasmic reticulum, spontaneous calcium release, and delayed after-depolarizations to explain arrhythmia in this model.^{23,47,48}

In Summary

Autophagy, a lysosomal-associated degradation of the cells' own constituents, plays an important role in the renewal and survival of cardiomyocytes. L2^{Δ6} hearts develop progressive cardiomyopathy because of abnormal lysosomal biogenesis, inability of mutant lysosomes to dock with autophagosomes, and failed autophagy. Accumulation of autophagy intermediates

and of undigested contents, causes myocyte injury, triggers hypertrophy, followed by cell death, myocardial fibrosis, and decreasing systolic function. Calcium dysregulation, abnormal calcium release, and increased sensitivity to catecholamine stimulation contribute to lethal arrhythmia in LAMP2 cardiomyopathy.

Limitations and Perspectives

By precisely introducing a “human” mutation into mouse genome, we generated a model of cardiomyopathy in Danon disease. These mice recapitulate the course of cardiomyopathy in human patients, as well as many of the histological and arrhythmic features. Important issues to be resolved are the function of the mutant protein LAMP2b, of the isoform LAMP2a involved in chaperon-mediated autophagy, as well as LAMP1 which apparently fails to compensate for LAMP2 deficiency. Studying the effect of pharmacological agents on autophagic flux, lysosomal function and calcium handling may clarify the link between LAMP2 defect and disease evolution. Most importantly, this model should be used to study potential therapies to modify the course of this lethal condition.

ARTICLE INFORMATION

Received August 4, 2020; accepted June 9, 2021.

Affiliations

Heart Institute, Hadassah Hebrew University Medical Center, Jerusalem, Israel (R.A., E.B.); Department of Genetics (R.A., H.W., J.G., L.W., T.K., D.A.C., J.G.S., C.E.S.) and Department of Pathology, Children's Hospital Boston (A.R.P.-A.), Harvard Medical School, Boston, MA; Division of Cardiology, Sheba Medical Centre and Tel Aviv University, Ramat Gan, Israel (M.A., D.Y.); Minneapolis Heart Institute Foundation, Minneapolis, MN (B.J.M.); Baylor Heart & Vascular Institute, Baylor University Medical Center, Dallas, TX (W.C.R.); and Howard Hughes Medical Institute and Cardiovascular Division, Brigham and Women's Hospital, Boston, MA (C.E.S.).

Sources of Funding

This work was supported by grants from Howard Hughes Medical Institute (C.E.S.), National Institutes of Health (J.G.S., C.E.S.), from the Machiah Foundation/Jewish Community Foundation Program (R.A.) and from the Chief Scientist Office, Israeli Ministry of Health (R.A.).

Disclosures

M.A. and D.Y. received a research support from Genzyme Corporation for a project entitled “Phenotype Modification and Developing Therapy in Cardiac Danon Disease.” The remaining authors have no disclosures to report.

Supplementary Material

Tables S1–S2

Figures S1–S5

REFERENCES

1. Nishino I, Fu J, Tanji K, Yamada T, Shimojo S, Koori T, Mora M, Riggs JE, Oh SJ, Koga Y, et al. Primary LAMP-2 deficiency causes X-linked vacuolar cardiomyopathy and myopathy (Danon disease). *Nature*. 2000;406:906–910. doi: 10.1038/35022604
2. Arad M, Maron BJ, Gorham JM, Johnson WH, Saul JP, Perez-Atayde AR, Spirito P, Wright GB, Kanter RJ, Seidman CE, et al. Glycogen

- storage diseases presenting as hypertrophic cardiomyopathy. *N Engl J Med*. 2005;352:362–372. doi: 10.1056/NEJMoa033349
3. Musumeci O, Rodolico C, Nishino I, Di Guardo G, Migliorato A, Aguenouz M, Mazzeo A, Messina C, Vita G, Toscano A. Asymptomatic hyperCKemia in a case of Danon disease due to a missense mutation in Lamp-2 gene. *Neuromuscul Disord*. 2005;15:409–411. doi: 10.1016/j.nmd.2005.02.008
 4. Yang Z, McMahon CJ, Smith LR, Bersola J, Adesina AM, Breinholt JP, Kearney DL, Dreyer WJ, Denfield SW, Price JF, et al. Danon disease as an underrecognized cause of hypertrophic cardiomyopathy in children. *Circulation*. 2005;112:1612–1617. doi: 10.1161/CIRCULATIONAHA.105.546481
 5. Maron BJ, Roberts WC, Arad M, Haas TS, Spirito P, Wright GB, Almquist AK, Baffa JM, Saul JP, Ho CY, et al. Clinical outcome and phenotypic expression in LAMP2 cardiomyopathy. *JAMA*. 2009;301:1253–1259.
 6. Brambatti M, Caspi O, Maolo A, Koshi E, Greenberg B, Taylor MRG, Adler ED. Danon disease: gender differences in presentation and outcomes. *Int J Cardiol*. 2019;286:92–98. doi: 10.1016/j.ijcard.2019.01.020
 7. Lavandero S, Chiong M, Rothermel BA, Hill JA. Autophagy in cardiovascular biology. *J Clin Invest*. 2015;125:55–64. doi: 10.1172/JCI73943
 8. Lieberman AP, Puertollano R, Raben N, Staugenhaupt S, Walkley SU, Ballabio A. Autophagy in lysosomal storage disorders. *Autophagy*. 2012;8:719–730. doi: 10.4161/auto.19469
 9. Marques ARA, Saftig P. Lysosomal storage disorders – challenges, concepts and avenues for therapy: beyond rare diseases. *J Cell Sci*. 2019;132:jcs221739. doi: 10.1242/jcs.221739. PMID: 30651381.
 10. Tanaka Y, Guhde G, Suter A, Eskelinen EL, Hartmann D, Lüllmann-Rauch R, Janssen PM, Blanz J, von Figura K, Saftig P. Accumulation of autophagic vacuoles and cardiomyopathy in LAMP-2-deficient mice. *Nature*. 2000;406:902–906. doi: 10.1038/35022595
 11. Saftig P, Tanaka Y, Lüllmann-Rauch R, von Figura K. Disease model: LAMP-2 enlightens Danon disease. *Trends Mol Med*. 2001;7:37–39. doi: 10.1016/S1471-4914(00)01868-2
 12. Stypmann J, Janssen PML, Prestle J, Engelen MA, Kögler H, Lüllmann-Rauch R, Eckardt L, von Figura K, Landgrebe J, Mleczko A, et al. LAMP-2 deficient mice show depressed cardiac contractile function without significant changes in calcium handling. *Basic Res Cardiol*. 2006;101:281–291. doi: 10.1007/s00395-006-0591-6
 13. Manso AM, Hashem SI, Nelson BC, Gault E, Soto-Hermida A, Villarruel E, Brambatti M, Bogomolovas J, Bushway PJ, Chen C, et al. Systemic AAV9.LAMP2B injection reverses metabolic and physiologic multi-organ dysfunction in a murine model of Danon disease. *Sci Transl Med*. 2020;12:eaax1744. doi: 10.1126/scitranslmed.aax1744. PMID: 32188720.
 14. Liu P, Jenkins NA, Copeland NG. A highly efficient recombineering-based method for generating conditional knockout mutations. *Genome Res*. 2003;13:476–484. doi: 10.1101/gr.749203
 15. Meyers EN, Lewandoski M, Martin GR. An Fgf8 mutant allelic series generated by Cre- and Flp-mediated recombination. *Nat Genet*. 1998;18:136–141. doi: 10.1038/ng0298-136
 16. Kupersmidt S, Yang T, Anderson ME, Wessels A, Niswender KD, Magnuson MA, Roden DM. Replacement by homologous recombination of the minK gene with lacZ reveals restriction of minK expression to the mouse cardiac conduction system. *Circ Res*. 1999;84:146–152.
 17. Karlen Y, McNair A, Perseguers S, Mazza C, Mermod N. Statistical significance of quantitative PCR. *BMC Bioinformatics*. 2007;8:131. doi: 10.1186/1471-2105-8-131
 18. Harms E, Kartenbeck J, Darai G, Schneider J. Purification and characterization of human lysosomes from EB-virus transformed lymphoblasts. *Exp Cell Res*. 1981;131:251–266. doi: 10.1016/0014-4827(81)90230-5
 19. Mas-Oliva J, Williams A, Nayler WG. Separation of isolated cardiac sarcolemma into inside-out and right-side-out vesicles by affinity chromatography. *Biochem Soc Trans*. 1979;7:950–952. doi: 10.1042/bst0070950
 20. McConnell BK, Fatkin D, Semsarian C, Jones KA, Georgakopoulos D, Maguire CT, Healey MJ, Mudd JO, Moskowitz IPG, Conner DA, et al. Comparison of two murine models of familial hypertrophic cardiomyopathy. *Circ Res*. 2001;88:383–389. doi: 10.1161/01.RES.88.4.383
 21. Semsarian C, Ahmad I, Giewat M, Georgakopoulos D, Schmitt JP, McConnell BK, Reiken S, Mende U, Marks AR, Kass DA, et al. The L-type calcium channel inhibitor diltiazem prevents cardiomyopathy in a mouse model. *J Clin Invest*. 2002;109:1013–1020. doi: 10.1172/JCI200214677
 22. Wolf CM, Arad M, Ahmad F, Sanbe A, Bernstein SA, Toka O, Konno T, Morley G, Robbins J, Seidman JG, et al. Reversibility of PRKAG2 glycogen-storage cardiomyopathy and electrophysiological manifestations. *Circulation*. 2008;117:144–154.
 23. Song L, Alcalai R, Arad M, Wolf CM, Toka O, Conner DA, Berul CI, Eldar M, Seidman CE, Seidman JG. Calsequestrin 2 (CASQ2) mutations increase expression of calreticulin and ryanodine receptors, causing catecholaminergic polymorphic ventricular tachycardia. *J Clin Invest*. 2007;117:1814–1823. doi: 10.1172/JCI31080
 24. Lim CC, Apstein CS, Colucci WS, Liao R. Impaired cell shortening and relengthening with increased pacing frequency are intrinsic to the senescent mouse cardiomyocyte. *J Mol Cell Cardiol*. 2000;32:2075–2082. doi: 10.1006/jmcc.2000.1239
 25. Teekakirikul P, Eminaga S, Toka O, Alcalai R, Wang L, Wakimoto H, Nayor M, Konno T, Gorham JM, Wolf CM, et al. Cardiac fibrosis in mice with hypertrophic cardiomyopathy is mediated by non-myocyte proliferation and requires Tgf- β . *J Clin Invest*. 2010;120:3520–3529. doi: 10.1172/JCI42028
 26. Nagata K, Liao R, Eberli FR, Satoh N, Chevalier B, Apstein CS, Suter TM. Early changes in excitation-contraction coupling: transition from compensated hypertrophy to failure in Dahl salt-sensitive rat myocytes. *Cardiovasc Res*. 1998;37:467–477. doi: 10.1016/S0008-6363(97)00278-2
 27. Christodoulou DC, Wakimoto H, Onoue K, Eminaga S, Gorham JM, DePalma SR, Herman DS, Teekakirikul P, Conner DA, McKean DM, et al. 5'RNA-Seq identifies Fhl1 as a genetic modifier in cardiomyopathy. *J Clin Invest*. 2014;124:1364–1370. doi: 10.1172/JCI70108
 28. Luptak I, Shen M, He H, Hirshman MF, Musi N, Goodyear LJ, Yan J, Wakimoto H, Morita H, Arad M, et al. Aberrant activation of AMP-activated protein kinase remodels metabolic network in favor of cardiac glycogen storage. *J Clin Invest*. 2007;117:1432–1439. doi: 10.1172/JCI30658
 29. Mizushima N, Yoshimori T. How to interpret LC3 immunoblotting. *Autophagy*. 2007;3:542–545. doi: 10.4161/auto.4600
 30. Behrends C, Sowa ME, Gygi SP, Harper JW. Network organization of the human autophagy system. *Nature*. 2010;466:68–76. doi: 10.1038/nature09204
 31. Rothermel BA, Hill JA. Autophagy in load-induced heart disease. *Circ Res*. 2008;103:1363–1369. doi: 10.1161/CIRCRESAHA.108.186551
 32. Seidman JG, Seidman C. The genetic basis for cardiomyopathy. *Cell*. 2001;104:557–567. doi: 10.1016/S0092-8674(01)00242-2
 33. Bhuiyan MS, Pattison JS, Osinska H, James J, Gulick J, McLendon PM, Hill JA, Sadoshima J, Robbins J. Enhanced autophagy ameliorates cardiac proteinopathy. *J Clin Invest*. 2013;123:5284–5297. doi: 10.1172/JCI70877
 34. Arad M, Benson DW, Perez-Atayde AR, McKenna WJ, Sparks EA, Kanter RJ, McGarry K, Seidman JG, Seidman CE. Constitutively active AMP kinase mutations cause glycogen storage disease mimicking hypertrophic cardiomyopathy. *J Clin Invest*. 2002;109:357–362. doi: 10.1172/JCI0214571
 35. Bijvoet AG, van de Kamp EH, Kroos MA, Ding JH, Yang BZ, Visser P, Bakker CE, Verbeet MP, Oostra BA, Reuser AJ, et al. Generalized glycogen storage and cardiomegaly in a knockout mouse model of Pompe disease. *Hum Mol Genet*. 1998;7:53–62. doi: 10.1093/hmg/7.1.53
 36. Matsuzawa F, Aikawa S, Doi H, Okumiyama T, Sakuraba H. Fabry disease: correlation between structural changes in alpha-galactosidase, and clinical and biochemical phenotypes. *Hum Genet*. 2005;117:317–328.
 37. Lim J-A, Meena NK, Raben N. Pros and cons of different ways to address dysfunctional autophagy in Pompe disease. *Ann Transl Med*. 2019;7:279. doi: 10.21037/atm.2019.03.51
 38. Macke H, Perdiz D, Lorin S, Codogno P, Poüs C. Autophagy and microtubules – new story, old players. *J Cell Sci*. 2013;126:1071–1080. doi: 10.1242/jcs.115626
 39. Xing R, Liu D, Cheng X, Tian X, Yan C, Han Y. MiR-207 inhibits autophagy and promotes apoptosis of cardiomyocytes by directly targeting LAMP2 in type 2 diabetic cardiomyopathy. *Biochem Biophys Res Commun*. 2019;520:27–34. doi: 10.1016/j.bbrc.2019.09.092
 40. Hashem SI, Perry CN, Bauer M, Han S, Clegg SD, Ouyang K, Deacon DC, Spinharney M, Panopoulos AD, Izpisua Belmonte JC, et al. Brief report: oxidative stress mediates cardiomyocyte apoptosis in a human model of danon disease and heart failure. *Stem Cells*. 2015;33:2343–2350. doi: 10.1002/stem.2015
 41. Hashem SI, Murphy AN, Divakaruni AS, Klos ML, Nelson BC, Gault EC, Rowland TJ, Perry CN, Gu Y, Dalton ND, et al. Impaired mitophagy facilitates mitochondrial damage in Danon disease. *J Mol Cell Cardiol*. 2017;108:86–94. doi: 10.1016/j.yjmcc.2017.05.007

42. Chi C, Leonard A, Knight WE, Beussman KM, Zhao Y, Cao Y, Londono P, Aune E, Trembley MA, Small EM, et al. LAMP-2B regulates human cardiomyocyte function by mediating autophagosome-lysosome fusion. *Proc Natl Acad Sci USA*. 2019;116:556–565. doi: 10.1073/pnas.1808618116
43. Colella M, Grisan F, Robert V, Turner JD, Thomas AP, Pozzan T. Ca²⁺ oscillation frequency decoding in cardiac cell hypertrophy: role of calcineurin/NFAT as Ca²⁺ signal integrators. *Proc Natl Acad Sci USA*. 2008;105:2859–2864. doi: 10.1073/pnas.0712316105
44. Carreira RS, Lee Y, Ghochani M, Gustafsson ÅB, Gottlieb RA. Cyclophilin D is required for mitochondrial removal by autophagy in cardiac cells. *Autophagy*. 2010;6:462–472. doi: 10.4161/auto.6.4.11553
45. Crompton M, Ellinger H, Costi A. Inhibition by cyclosporin A of a Ca²⁺-dependent pore in heart mitochondria activated by inorganic phosphate and oxidative stress. *Biochem J*. 1988;255:357–360.
46. Kim SJ, Iizuka K, Kelly RA, Geng YJ, Bishop SP, Yang G, Kudej A, McConnell BK, Seidman CE, Seidman JG, et al. An alpha-cardiac myosin heavy chain gene mutation impairs contraction and relaxation function of cardiac myocytes. *Am J Physiol*. 1999;276:H1780–H1787.
47. Knollmann BC, Chopra N, Hlaing T, Akin B, Yang T, Etensohn K, Knollmann BEC, Horton KD, Weissman NJ, Holinstat I, et al. Casq2 deletion causes sarcoplasmic reticulum volume increase, premature Ca²⁺ release, and catecholaminergic polymorphic ventricular tachycardia. *J Clin Invest*. 2006;116:2510–2520. doi: 10.1172/JCI29128
48. Lehnart SE, Terrenoire C, Reiken S, Wehrens XHT, Song L-S, Tillman EJ, Mancarella S, Coromilas J, Lederer WJ, Kass RS, et al. Stabilization of cardiac ryanodine receptor prevents intracellular calcium leak and arrhythmias. *Proc Natl Acad Sci USA*. 2006;103:7906–7910. doi: 10.1073/pnas.0602133103

Supplemental Material

Table S1. RNA expression in wild-type and L2^{Δ6} hearts.

Gene category	All genes	L2 ^{Δ6} > WT	P	L2 ^{Δ6} < WT	P
All RNAs	31920	1278 (4%)		707 (2.2%)	
Autophagy markers	793	62 (7.8%)	<0.001	15 (1.9%)	0.54
Apoptotic markers	1252	85(6.8%)	<0.001	21(1.7%)	0.2

Percentages represent gene counts in each category out of the total gene counts. A change in gene expression was defined by at least ≥ 1.5 or < 0.67 ratio in the read count (for increase or decrease respectively).

L2^{Δ6} > WT, number of genes expressed in L2^{Δ6} tissue at a higher level than in wildtype (WT) tissue. L2^{Δ6} < WT, number of genes expressed in L2^{Δ6} tissue at a lower level than in wild type (WT) tissue. P values - comparison of the percent change between all RNAs and markers of either Autophagy or Apoptosis.

All RNAs, reflects RNAs identified as expressed by RNAseq as described by Christodoulou et al²⁷.

Autophagy markers is a set of autophagy-associated proteins collected from <http://www.tanpaku.org/autophagy/list/GeneList.html>. Apoptotic signaling pathway genes collected from <http://www.informatics.jax.org/go/term/GO:0097190>.

Specific details of the genes and the fold changes in expression are available upon request.

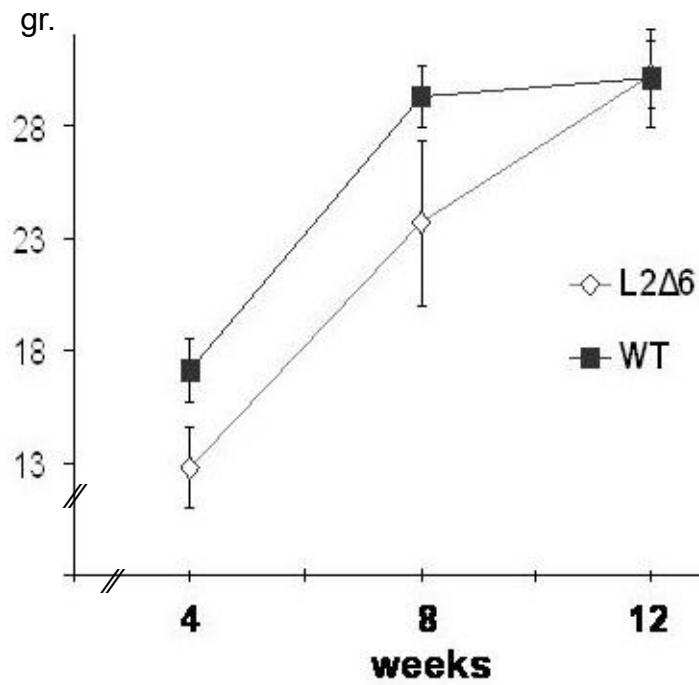
The full results of the transcriptome analysis are provided at <https://www.ncbi.nlm.nih.gov/geo/query/acc.cgi?acc=GSE166731> (GEO accession number GSE166731).

Table S2. Autophagy and apoptosis related genes showing the greatest change in expression in hearts of L2^{Δ6} mice.

	Gene ID	Gene description	Fold change (L2^{Δ6}/WT)	WT normalized reads	Regulation	P-value
Autophagy	<i>Tlr13</i>	toll-like receptor 13	16.30	0.12	up	<0.0001
	<i>Crocc</i>	ciliary rootlet coiled-coil	3.97	0.83	up	0.0003
	<i>Bcl2l1</i>	BCL2-like 1	3.75	157.54	up	<0.0001
	<i>Sgk1</i>	serum/glucocorticoid regulated kinase 1	3.41	31.15	up	<0.0001
	<i>Ddit4</i>	DNA-damage-inducible transcript 4	3.40	81.68	up	<0.0001
	<i>Rcan1</i>	regulator of calcineurin 1	3.26	103.20	up	<0.0001
	<i>Tecpr1</i>	tectonin beta-propeller repeat containing 1	3.12	25.56	up	<0.0001
	<i>Il18r1</i>	interleukin 18 receptor 1	0.12	16.00	down	0.0005
	<i>Phkg1</i>	phosphorylase kinase gamma 1	0.29	267.00	down	<0.0001
	<i>Alpl</i>	alkaline phosphatase	0.31	146.00	down	<0.0001
Apoptosis	<i>Bid</i>	BH3 interacting domain death agonist	49.00	0.00	up	<0.0001
	<i>Lcn2</i>	lipocalin 2	26.66	6.90	up	0.0005
	<i>S100a9</i>	S100 calcium binding protein A9	16.87	0.59	up	0.0003
	<i>Bdkrb2</i>	bradykinin receptor, beta 2	10.22	0.36	up	<0.0001
	<i>Ankrd2</i>	ankyrin repeat domain 2	9.27	0.36	up	<0.0001
	<i>Plaur</i>	plasminogen activator	5.43	0.71	up	<0.0001
	<i>Cdkn1a</i>	cyclin-dependent kinase inhibitor 1A	4.92	85.01	up	<0.0001
	<i>Pawr</i>	PRKC, apoptosis	4.03	1.19	up	<0.0001
	<i>Trp63</i>	transformation related protein 63	0.08	4.52	down	<0.0001
	<i>Cx3cr1</i>	chemokine (C-X3-C motif) receptor 1	0.20	3.45	down	<0.0001

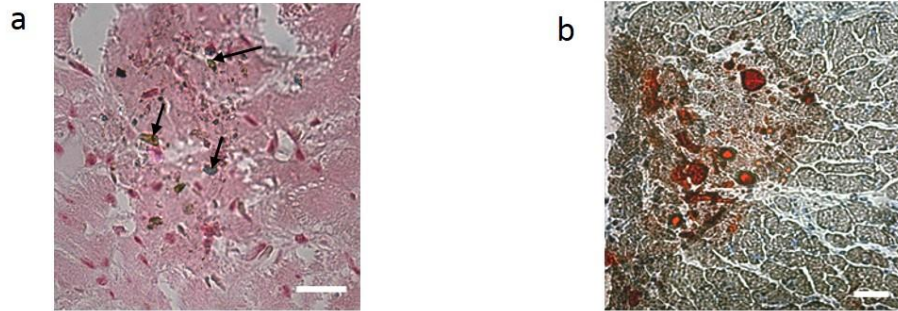
Ten genes which changed most (in either direction) are shown in each category. RNAseq libraries were constructed from hearts of adult L2^{Δ6} and WT mice and data were analyzed as described²⁷.

Figure S1. Average weight of 10 WT and 10 L2^{Δ6} mice at 4, 8, and 12 weeks.



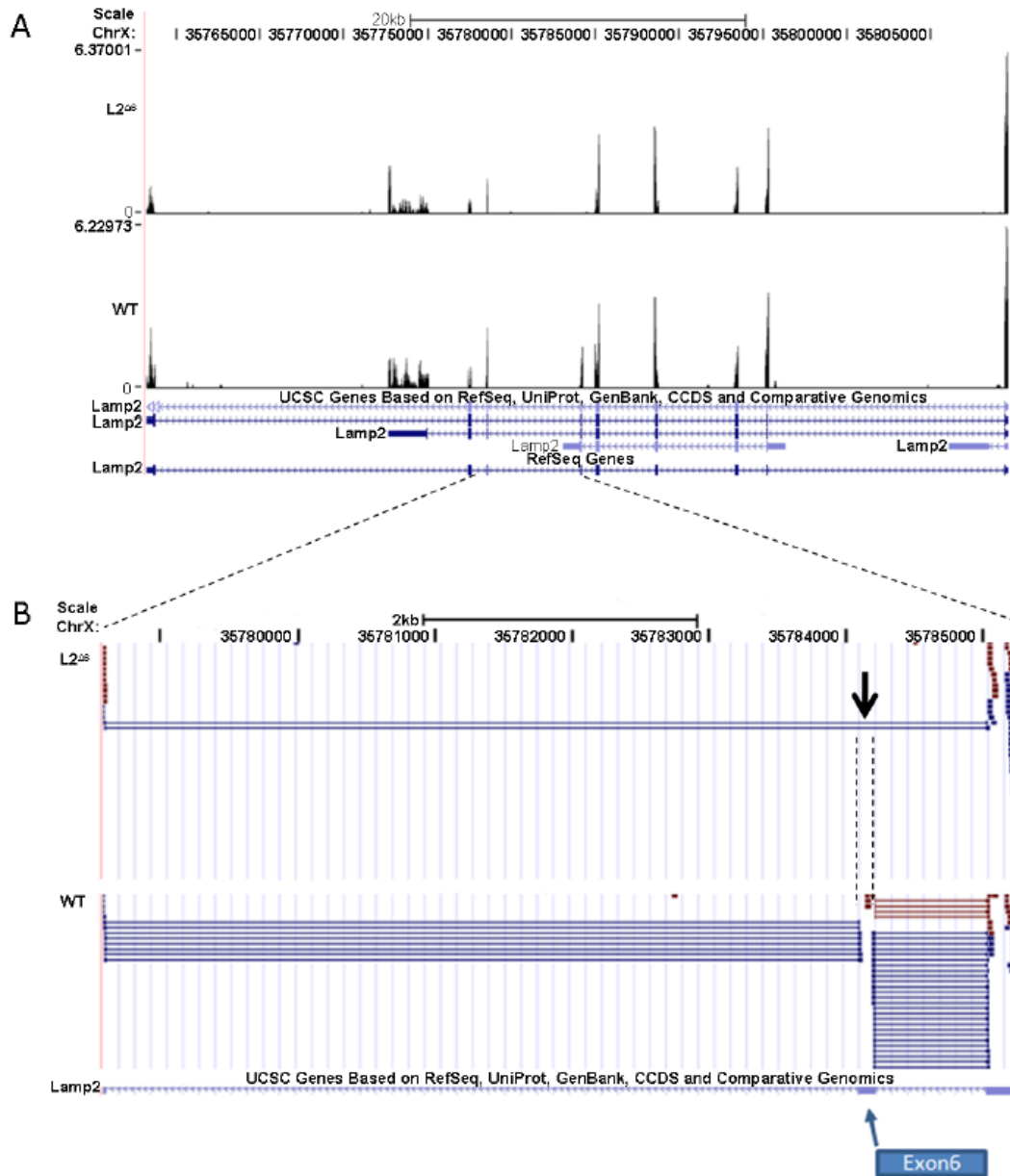
The L2^{Δ6} had a lower body weight at 4 weeks but the differences were not anymore apparent at 12 weeks age.

Figure S2. Cell death in L2^{Δ6} hearts.



(a) Von Kossa stains of 40-week old L2^{Δ6} hearts show dystrophic calcification (arrows) consistent with necrosis (scale bar = 50 μ m). (b) Oil-red-O staining of frozen section of 40 week old L2^{Δ6} heart showing fat depositions (in red) within the myocardium. Scale bar = 50 μ m.

Figure S3. RNAseq analysis.



RNAseq analysis is demonstrated by the assessment of *Lamp2* RNA expression in WT and *L2^{A6}* hearts.

A) Screen shot of UCSC Genome Browser custom tracks

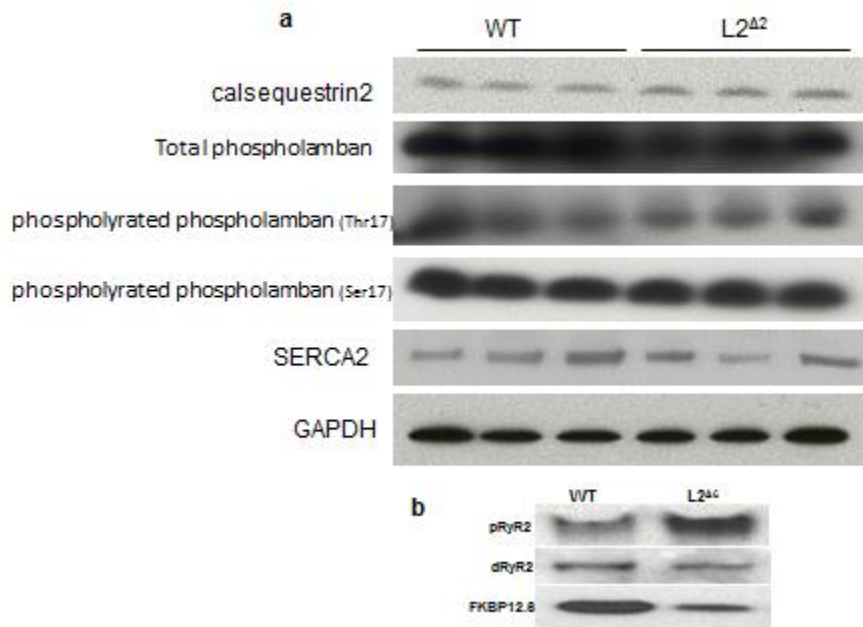
(WIG files; [http://genome.ucsc.edu/cgi-](http://genome.ucsc.edu/cgi-bin/hgTracks?hgS_doOtherUser=submit&hgS_otherUserName=JonSeidman&hgS_other)

[bin/hgTracks?hgS_doOtherUser=submit&hgS_otherUserName=JonSeidman&hgS_other](http://genome.ucsc.edu/cgi-bin/hgTracks?hgS_doOtherUser=submit&hgS_otherUserName=JonSeidman&hgS_other)

UserSessionName=Lamp2_mm9), displaying the LAMP2 gene and normalized number of DNA sequence reads per million in L2^{Δ6} and wildtype LV RNAseq libraries (see Methods). RNAseq libraries were constructed from 2 micrograms of total left ventricular RNA pooled from two mice of each genotype (see Methods). Four different LAMP2 isoforms are presented in the UCSC gene list. LAMP2 extends from exon 1 (right) to exon 10 (left). Note that 5' exons are more highly represented in this RNAseq data than 3' exons because of the method used for RNAseq library construction (our unpublished results).

B) Screen shot from custom tracks (BAM files) of UCSC Genome Browser displaying DNA sequence reads obtained from L2^{Δ6} and WT LV RNAseq libraries between exon 5 and 7. Exon 6 is skipped in L2^{Δ6} RNA as predicted by PCR analysis (black arrow).

Figure S4. Expression of key calcium handling proteins in L2^{Δ6} hearts.

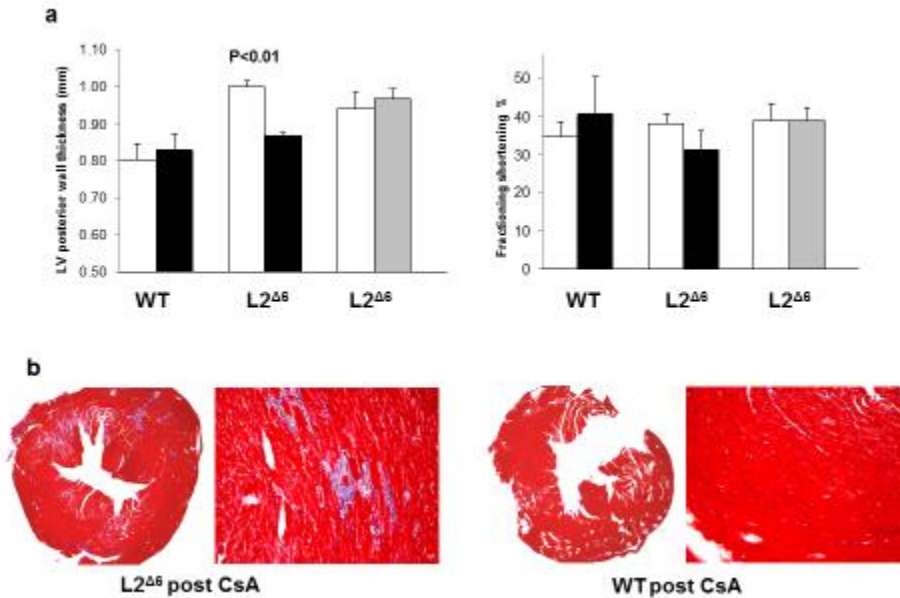


a) Western blot analysis of Calsequestrin2, Phospholamban (both total and the phosphorylated forms) and the cardiac sarcoplasmic reticulum Ca²⁺-ATPase (SERCA2) revealed no differences in the expression between wild type and L2^{Δ6}.

b) Increased expression of phosphorylated RyR2 and decreased expression of FKBP12.6 (calstabin) in L2^{Δ6} hearts. See also figure 5.

All analyses were done on sarcoplasmic reticulum fraction of ventricular muscle extracts.

Figure S5. Cyclosporin A inhibits hypertrophy in L2^{Δ6} hearts.



a) Left ventricular posterior wall thickness (left panel) and left ventricular fractional shortening (right panel) before (white bars) and after (black bars) 2 weeks of treatment with Cyclosporin A (CsA) in L2^{Δ6} and wild type (WT) mice (two subcutaneous injections of

15 mg/kg in PBS daily). The gray bars represent control age-matched L2^{Δ6} mice that were followed for 2 weeks without treatment (mean \pm SEM, $n=3$ /group, age at examination 32 weeks). Left ventricular posterior wall thickness was significantly reduced in treated L2^{Δ6} hearts compared to untreated ($p < 0.01$). No significant differences were found in the interventricular septum thickness, left ventricular dimension or fractional shortening b) Histology section stained with Masson's trichrome for fibrosis (in blue) of L2^{Δ6} and wild type hearts assessed two weeks after treatment with CsA. The amount of fibrosis in L2^{Δ6} hearts was comparable to untreated hearts (see Figure 1 for reference). There was no significant fibrosis in age-matched wild type hearts before or after treatment (data not shown).